Proceedings of the Canadian Society for Mechanical Engineering International Congress 2021
CSME Congress 2021
June 27-30, 2021, Charlottetown, PE, Canada

Synthetic Jet Development for Wall Jet Flow Control

Bonnie Sim
Department of Mechanical Engineering
University of New Brunswick
Fredericton, Canada
bonnie.sim@unb.ca

Kieran Ellis
Department of Mechanical Engineering
University of New Brunswick
Fredericton, Canada
kieran.ellis@unb.ca

Joseph W. Hall
Department of Mechanical Engineering
University of New Brunswick
Fredericton, Canada
jwhall@unb.ca

***Abstract*—The design and construction of synthetic jet actuators for use in active flow control of a turbulent three-dimensional wall jet was investigated experimentally. Seven actuator designs of varying cavity depth and channel height were evaluated based on hot-wire velocity measurements, maximum RMS velocity outputs, and momentum coefficients. Initially, the synthetic jet actuators were driven with sinusoidal frequency sweeps from 10 Hz to 1510 Hz to identify frequencies associated with the strongest velocity output. For each actuator, momentum coefficients were calculated from sinusoidal inputs at the frequencies that produced the strongest jets. Evaluation of these tests showed that the most successful synthetic jet actuator had a cavity depth of 2 mm and channel height of 1.5 mm; it produced the strongest velocity output with momentum coefficients from 0.03-0.05 at input frequencies of 1100-1150 Hz. Synthetic jet actuators capable of providing these momentum coefficients have been shown from the literature to achieve flow control.**

***Index Terms*—Synthetic jets, active flow control, three-dimensional wall jets, unsteady wall pressure**

I. Introduction

Three-dimensional wall jets are flows that exit through finite-width openings and develop tangentially to a surface. These jets are unique because they exhibit a large lateral growth rate in the far-field, approximately five to eight times larger than the growth rate of the jet normal to the wall [1]–[4]. The mechanisms that cause this difference in growth rates are not fully understood. However, it is known that strong mean turbulence generated secondary flows, which draw mean flow downward and eject it laterally outward, cause the large lateral growth in the wall jet [3]–[5].

Many researchers [5]–[17] have found that secondary flow is linked to the passage of coherent structures in the wall jet and have developed coherent structure models. Most research postulates that these structures are large horseshoe-like vortices, which are likely asymmetric about the jet centreline [14], [16], [17], and are responsible for a downward and lateral ejection of the flow [15], [16].

Recent studies by Sim and Hall [18], [19] used measurements of unsteady wall pressure to show that there were organized angled regions of pressure fluctuations in the wall jet. Subsequent Proper Orthogonal Decomposition and low-order reconstructions of the unsteady wall pressure indicated that specific modes were linked to leftward and rightward meandering of the wall jet [19]. Amplifying these modes could amplify the meandering of the wall jet, thereby increasing the lateral spread of the wall jets. To amplify these modes, active flow control could be applied to the wall jet. Active flow control involves altering the flow state of a system through the addition of energy [20]. Therefore, targeting the modes associated with wall jet meandering through the addition of energy to the flow could amplify jet development.

Active flow control can be implemented in several ways, however, previous studies [21], [22] show that synthetic jets can alter the development of many flows, including wall jets. Glezer and Amitay [23] defined synthetic jets or zero-net mass-flux jets as pulsed jets formed from the fluid of the system. Synthetic jets are formed by the periodic suction and expulsion of the working fluid across an orifice or nozzle [23], [24]. Therefore, the synthetic jets do not add mass to a system but can add momentum flux, which can modify a flow field significantly.

In previous studies, synthetic jets have been shown to alter the flow fields of free jets [25]–[27] to an experimentally significant degree. Perez, et al, [21], [22] applied a synthetic jet array to a wall jet nozzle and found that lower actuation frequencies (30 Hz, 60 Hz, and 120 Hz) enhanced the lateral width of the wall jet. Like Perez, et al, [21], [22], the future aim of this study is to utilize synthetic jets in a circumference around the outlet of the wall jet to provide in-phase, active forcing at frequencies of interest. Sim and Hall [18], [19] identified low frequency sweeps in the wall jet, within the range tested by Perez, et al; if the jet could be forced at these frequencies, then these low frequency sweeps could be attenuated, thereby increasing the lateral growth of the jet. The aim of this study is to develop synthetic jet actuators with the ultimate goal of altering the growth of wall jet through active flow control using a synthetic jet array.

II. Experimental methodology

To meet the objectives for this current study, the development of the synthetic jets was explored experimentally. The

The authors are grateful for funding by the Natural Sciences and Engineering Research Council of Canada (NSERC), the New Brunswick Innovation Foundation (NBIF), and the International Society of Automation Process Measurement and Control Division (ISA PMCD).

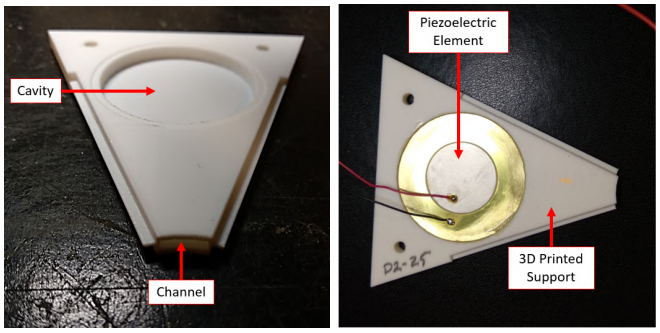

(a) (b)

Fig. 1: The (a) 3D printed support for the piezoelectric buzzer and (b) the combined piezoelectric buzzer and 3D printed support.

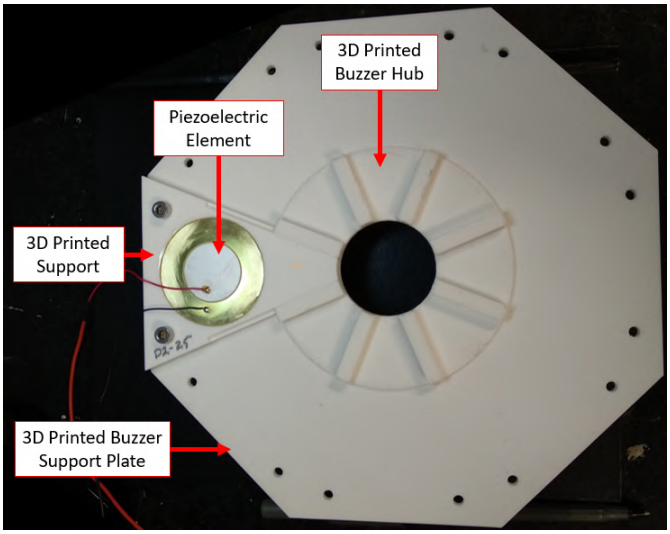

Fig. 2: The 3D printed buzzer hub with one synthetic jet actuator in place.

synthetic jet consists of two main components: the piezoelectric element and the stereolithography 3D-printed holder for the piezoelectric element with the synthetic jet cavity and channel printed in it (colloquially known as buzzers), as shown in Fig. 1a. To investigate and characterize the synthetic jet actuators, the velocity output was experimentally measured using hot-wire anemometry.

The hot-wire anemometer probe was manufactured by Nan Gao and used in conjunction with a Dantech 56C17 CTA Bridge. The hot-wire probe was set up in accordance to the published guidelines [28] and the Dantec bridge was balanced as per the outlined steps [29]. The hot-wire bridge was a constant temperature bridge that adjusted the current running through the hot-wire to maintain a constant resistance [29]. The overheat ratio was set to 1.8 [30] and the bridge settings were kept constant throughout the synthetic jet characterization.

The piezoelectric buzzers were PUI piezoelectric ceramic in a 44-mm-diameter brass casing and had a resonant frequency of 1200 Hz $\pm$ 200 Hz [31]. Buzzer selection was based on their ability to be driven with a strong input signal (30 V_{pp}) [31] and compatibility with the existing support design. It was immediately apparent that the type and amount of adhesive used to affix each piezoelectric element to its support had an impact on the frequency response of the buzzer, and its resulting synthetic jet. Initially, a LePage ethyl cyanoacrylate super glue [32] was used, however, because of the applicator, it was difficult to control the quantity of glue applied to the piezoelectric buzzer, which caused large variation in its frequency response. Because of the variability in response, a polyurethane Gorilla^{TM} glue [33] was used, which resulted in a more flexible seal, and, therefore, a higher frequency response.

The piezoelectric elements were driven by an in-house built power supply and amplifier system to maximize their outputs. The preliminary goal was to find eight consistent buzzers that could create uniform powerful synthetic jets. The synthetic jet actuators will be encased in a 3D printed hub that will space them equidistant around the circumference of the jet nozzle, as shown in Fig. 2. The design for the 3D printed supports for the piezoelectric elements were based off previously completed work [34] and [35], therefore, the current designs were kept similar with the option to reassess based on evaluation of the results.

A number of channel heights and cavity depths were tested to determine the optimal buzzer geometry. A typical 3D printed buzzer support component is shown in Fig. 1a, with the synthetic jet cavity and channel indicated on it. It was found that the quality and method of 3D printing greatly impacted the accuracy of the cavity and channel dimensions, the porosity and seal of the buzzer support, and the frequency response of the buzzer. Therefore, to ensure consistency, the piezoelectric supports were printed in the same orientation with the highest quality print setting using the same material.

The buzzer supports consisted of a shallow circular inset of 44 mm that was concentric to a circular cavity with a diameter of 40.1 mm, which allowed the 44-mm piezoelectric buzzer to fit tightly before adhesive was applied, as shown in Fig. 1b. The channel width and length were constant across all support designs. The channel width was 8.0 mm. As evident in Fig. 1a, there was a radius of curvature to the buzzer supports which ensured a consistent circumference in the support hub to match the nozzle outlet. Therefore, the channel length was taken as the average length across this radius of curvature and was calculated to be 32.36 mm. The channel directed the flow of air when the piezoelectric buzzer was pulsed to create the synthetic jet. The cavity depths and channel heights were varied to determine the most powerful synthetic jets, which are summarized in Table I. The configuration designation indicates different printing and geometry iterations and were so designated for experimental tracking.

The hot-wire was positioned as shown in Fig. 3 and kept in the same lateral and vertical position across all tests but was adjusted horizontally to maximize the velocity of the synthetic jet at the outlet; the hot-wire was aligned with the channel

TABLE I: The geometric parameters for piezoelectric buzzer supports

Configuration Designation	Cavity Depth [mm]	Channel Height [mm]
B1	3.8	2.25
D1	2.2	2.0
D2	2.0	1.5
D3	2.0	1.0
E1	3.8	2.0
E2	3.8	1.5
E3	3.8	1.0

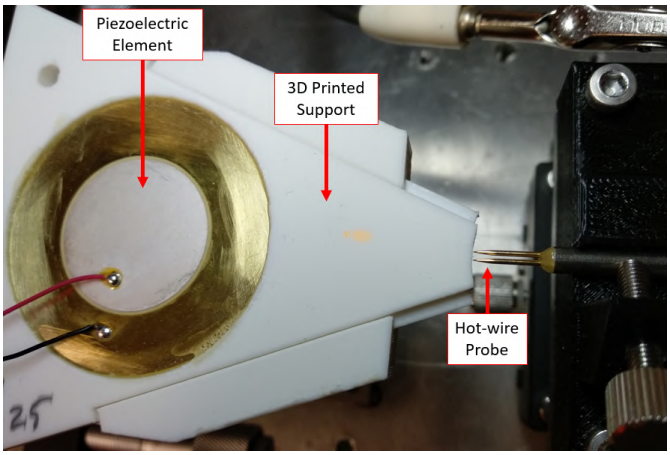

Fig. 3: The hot-wire and synthetic jet configuration used to test and calibrate the synthetic jets.

opening of the synthetic jet. The hot-wire was sampled at 20 kHz and 10 seconds of data was recorded (2×10^5 data points) for each frequency tested. Depending on the frequency of interest, there was a minimum of 1500 cycles of the signal measured by the hot-wire anemometer.

III. Results and Analysis

The first goal was to ascertain which of the seven geometries provided the strongest synthetic jets. Initially, the cavity resonance (f_c) was first estimated as using a Helmholtz resonance approach [36], as given by:

$$f_c = \frac{a}{2\pi}\sqrt{\frac{A_{SJ}}{l_{\text{channel}} \times V_{\text{cavity}}}} \tag{1}$$

where a is the speed of sound in air, A_{SJ} is the area of the synthetic jet opening, l_{channel} is the length of the channel, and V_{cavity} is the volume of the cavity. Excitation at the cavity frequency could produce stronger synthetic jets. Table II summarizes the theoretical resonance frequency based on cavity height and channel depth. However, it has been found [36] that synthetic jet actuators designed similarly to those in this study would operate as quarter-wave resonators instead of Helmholtz resonators with the quarter-wave resonance frequency (f_c) defined as:

$$f_c = \frac{a}{4(D_{\text{cavity}} + l_{\text{channel}})} \tag{2}$$

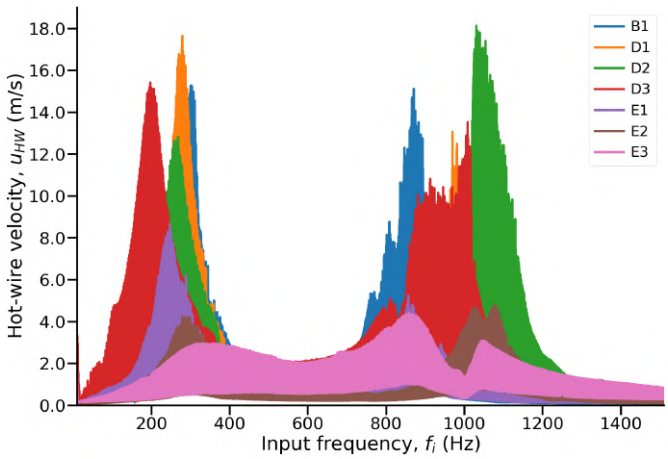

Fig. 4: Hot-wire velocity measurements for each synthetic jet configuration in response to a sinusoidal frequency sweep from 10 Hz to 1510 Hz.

where D_{cavity} is the diameter of the cavity with all other quantities as previously defined. Since all the actuators have the same cavity diameter and same channel length, their quarter-wave resonance frequency would be the same at approximately 1187 Hz.

To assess the accuracy of the cavity resonance, as well as ascertain the cavity and channels that produced the strongest synthetic jets, each piezoelectric element and support configuration was swept with a sinusoidal signal that ranged from 10 Hz to 1510 Hz (a range of 1500 Hz); 10 Hz was selected because it was at the low end of fluctuations that the microphones used to measure unsteady wall pressure in the jet could detect [37], while 1510 Hz ensured that the reported resonant frequency of the piezoelectric elements (1200 ± 200 Hz [31]) would be captured. The hot-wire probe was used to measure the resulting velocity output of the synthetic jets from these chirp signals. The frequency sweep demonstrated which excitation frequencies had the highest response and output from the buzzers, therefore producing the strongest synthetic jets. A comparison plot of the hot-wire velocity measurements of these chirp signals for each synthetic jet is shown in Fig. 4.

From initial analysis of the chirp signal, it appeared that all buzzers exhibited a lower frequency peak and a higher frequency peak, which varied slightly depending on the geometry of the support. The lower frequency peak was between 200 Hz and 300 Hz, while the higher frequency peak was between 800 Hz and 1200 Hz. Both peaks were inconsistent with predicted cavity resonance frequencies. However, the higher frequency peak was more consistent with the quarter-wave resonance frequency [36], as well as the stated resonance frequency for the piezoelectric element [31].

The chirp signal also showed that the velocity magnitude varied greatly between the support geometry configuration. Velocity measurements the B- and D-series actuators indicated that they could potentially produce strong synthetic jets. Both

TABLE II: Cavity resonance, RMS velocity, and momentum coefficients for the synthetic jet actuators

Configuration Designation	Cavity Resonance [Hz]	RMS Velocity [m/s]	Momentum Coefficients
B1	589	< 12.5	0.042
D1	766	< 12.0	0.036
D2	663	< 14.6	0.039
D3	542	< 9.5	0.011
E1	556	< 5.6	0.0076
E2	481	< 3.4	0.0021
E3	393	< 3.25	0.0013

frequency peaks for the B- and D-series were greater than 14 m/s, with some trials approaching 20 m/s. The D-series exhibited a high-frequency peak that was higher in frequency than the high-frequency peak observed in the B1 response, which is possibly a characteristic of the cavity depth.

Conversely, the E-series of buzzers, as defined in Table I, all had a cavity depth of 3.8 mm and seemed to generate the weakest synthetic jets. The configuration of cavity depth and channel height in these actuators resulted in peaks that were not as well-defined as the other support geometries. The synthetic jets also appeared to only be able to produce peak velocities less than approximately 5 m/s.

However, to obtain a better representation of the synthetic jet response, each support geometry was tested by sending a sinusoidal signal at the strongest excitation frequencies measured from the chirp signal tests. The first metric that the synthetic jets were characterized with was the maximum root-mean-square (RMS) velocity measured from the sinusoidal signal input, which are summarized in Table II. To support the findings from the analysis of the RMS velocity, the momentum coefficients were also estimated for each support geometry configuration. The momentum coefficient (C_μ) was calculated with [38], [39]:

$$C_\mu = \Sigma_i(\rho U_{\text{RMS}}^2 A_i)/(1/2\rho U_j^2 A_j) \tag{3}$$

where A_i is the area of the ith slot, A_j is the area of the wall jet nozzle, U_{RMS} is the RMS velocity of the synthetic jet, and U_j is the nominal outlet velocity of the wall jet. Since there are eight synthetic jets, $1 \leq i \leq 8$. Based on previous testing and the microphone sensitivity to low pressure fluctuations, the jet exit velocity was set at $U_j = 30$ m/s for momentum coefficient estimation. The estimated momentum coefficients for the maximum velocity output for each synthetic jet are summarized in Table II. The literature shows that C_μ of 0.01-0.02 [24], [39] is strong enough to alter the development of a flow field.

It was immediately evident that the E-series produced weaker jets, where the RMS velocity for the strongest frequencies was less than 6 m/s for all three configurations, with E2 and E3 performing exceptionally poorly with RMS velocities of < 3.5 m/s. The B- and D-series performed better, with synthetic jets having a maximum RMS velocity between 9.5 m/s and 14.6 m/s depending on the input frequency. Of the D-series, D2 produced the strongest synthetic jet, with B1 and D1 also exhibiting strong synthetic jets. From the

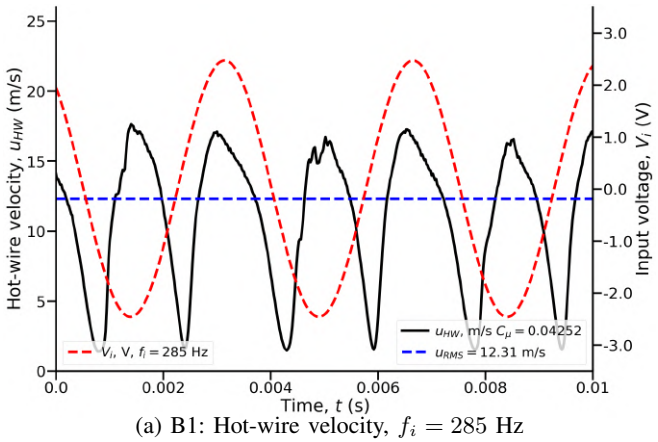

(a) B1: Hot-wire velocity, $f_i = 285$ Hz

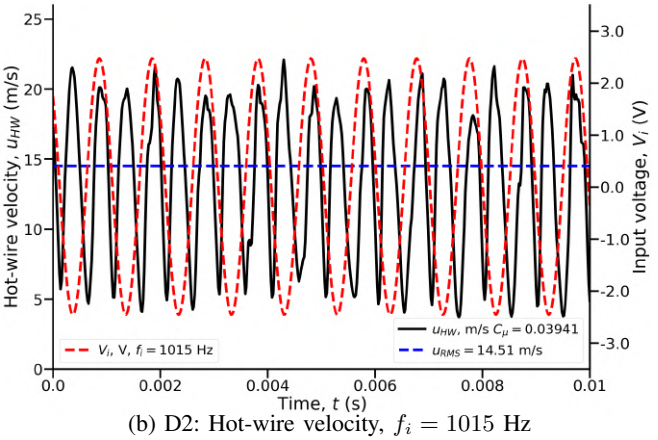

(b) D2: Hot-wire velocity, $f_i = 1015$ Hz

Fig. 5: Hot-wire velocity measurements and input signals for synthetic jet configurations (a) B1 and (b) D2 showing their strongest response.

specific sinusoidal inputs, the RMS velocities and momentum coefficients showed that the synthetic jets produced with the D2 configuration were stronger at higher frequencies (> 10 kHz), while the B1 and D1 configuration produced jets that were strongest at at frequencies < 300 Hz. With repeated testing, B1 and D2 consistently produced the strongest jets, therefore, they were examined further.

Fig. 5 shows plots for the strongest synthetic jets measured from the B1 5a and D2 5b actuators. Both actuators produced synthetic jets of relatively high velocity, however the frequency inputs required to achieve these jets were quite different. The B1 configuration worked best at a lower frequency of 285 Hz, while the D2 configuration produced the strongest synthetic jet at 1015 Hz. Since D2 performed better at frequencies closer to the resonant frequency of the piezoelectric element and produced a stronger synthetic jet, it was selected for further study.

Eight synthetic jet actuators are required to implement active control on the wall jet given the current actuator array hub about the circumference of the nozzle. Therefore, eight uniform actuators with replicable synthetic jet responses were needed. Since there was variation in the piezoelectric

elements and the 3D printed support geometries, obtaining these uniform synthetic jets necessitated the construction of many actuators. During this process, refinement of the gluing procedure and the change in adhesive occurred. These refinements resulted in stronger synthetic jets at higher frequencies ($\geq$ 1100 Hz) using the D2 geometry configuration, which is evident when comparing the measured velocity between a preliminary D2 actuator in Fig. 5b and the more recently constructed D2 actuators in Figs. 6a and 6c.

Fig.6 compares the velocity response and power spectra for two D2 actuators subjected to excitation at 1100 Hz. Both actuators exhibit relatively high RMS velocities ($\geq$ 16 m/s) and momentum coefficients ($C_\mu \approx 0.049$), as indicated on the plots in Figs. 6a and 6c. The power spectra, shown in Figs. 6b and 6d, both exhibit one dominant peak at 1100 Hz, indicating that the synthetic jets are strongly actuated at the input frequency. Several other actuators of the D2 design have been tested and have exhibited strong velocity outputs at frequencies between 1100 Hz and 1150 Hz producing synthetic jets with momentum coefficients $C_\mu \geq 0.03$. Since these synthetic jets have momentum coefficients larger than those known to alter flow development [24], [39], they are promising in their ability to potentially alter the development of the wall jet.

IV. Conclusions

The design and effectiveness of synthetic jets were investigated experimentally. Hot-wire velocity measurements were conducted for several actuator designs where cavity depth and channel height were varied. The strongest synthetic jet actuator design was selected based on maximum RMS velocity output from sinusoidal input signals. The most promising design had a cavity with a diameter of 40.1 mm and a depth of 2.0 mm, and a corresponding channel depth of 1.5 mm. Based on a jet velocity of $U_j = 30$ m/s, the momentum coefficients for these synthetic jets were between 0.03 and 0.05 for input sinusoidal signals of 1100-1150 Hz at 30 V_{pp}. Their momentum coefficients will provide sufficient control for active flow control [24], [39].

References

[1] P. Bakke, "An experimental investigation of a wall jet," *J. Fluid Mech.*, vol. 2, no. 5, pp. 467–472, 1957.

[2] B. E. Launder and W. Rodi, "The turbulent wall jet," *Prog. Aerosp. Sci.*, vol. 19, pp. 81 – 128, 1979.

[3] B. E. Launder and W. Rodi, "The turbulent wall jet measurements and modeling," *Ann. Rev. Fluid Mech.*, vol. 15, no. 1, pp. 429–459, 1983.

[4] T. J. Craft and B. E. Launder, "On the spreading mechanism of the three-dimensional turbulent wall jet," *J. Fluid Mech.*, vol. 435, no. 1, pp. 305–326, 2001.

[5] L. Namgyal and J. W. Hall, "Reynolds stress distribution and turbulence generated secondary flow in the turbulent three-dimensional wall jet," *J. Fluid Mech.*, vol. 800, pp. 613–644, 2016.

[6] H. Matsuda, S. Iida, and M. Hayakawa, "Coherent structures in a three-dimensional wall jet," *J. Fluids Eng.*, vol. 112, no. 4, p. 462, 1990.

[7] D. Ewing and A. Pollard, "Evolution of the large scale motions in a three-dimensional wall jet," in *28th Fluid Dyn. Co-located Conf.*, American Institute of Aeronautics and Astronautics, June 1997.

[8] D. Ewing, A. Benaissa, A. Pollard, J. Citriniti, H. Abrahamsson, and L. Lofdahl, "Contribution of large structures to the anisotropic spread rate in a wall jet issuing from a round nozzle," in *Tenth Int. Symp. Transp. Phenom. Therm. Sci. Process Eng.*, 1997.

[9] H. Sun and D. Ewing, "The development of three-dimensional wall jet," in *Proc. 48th Ann. Conf. Canadian Aeronautics and Space Institute*, (Toronto, Canada), 2002.

[10] H. Sun and D. Ewing, "Effect of initial and boundary conditions on development of three-dimensional wall jets," AIAA paper 2002-0777, McMaster University, 2002.

[11] J. W. Hall and D. Ewing, "On the dynamics of the large-scale structures in round impinging jets," *J. Fluid Mech.*, vol. 555, pp. 439–438, 2006.

[12] J. W. Hall and D. Ewing, "A combined spatial and temporal decomposition of the coherent structures in the three-dimensional wall jet," in *44th AIAA Aerospace Sciences Meeting and Exhibit*, (Reno, NV USA), pp. 1–18, January 2006.

[13] J. W. Hall and D. Ewing, "Three-dimensional turbulent wall jets issuing from moderate-aspect-ratio rectangular channels," *AIAA J.*, vol. 45, no. 6, pp. 1177–1186, 2007.

[14] J. W. Hall and D. Ewing, "The asymmetry of the large-scale structures in turbulent three-dimensional wall jets exiting long rectangular channels," *J. Fluids Eng.*, vol. 129, no. 7, pp. 929–941, 2007.

[15] J. W. Hall and D. Ewing, "Spectral linear stochastic estimation of the turbulent velocity in a square three-dimensional wall jet," *J. Fluids Eng.*, vol. 132, no. 5, pp. 1–9, 2010.

[16] L. Namgyal and J. W. Hall, "Coherent streamwise vortex structures in the near-field of a the three-dimensional wall jet," *J. Fluids Eng.*, vol. 135, no. 6, pp. 1–7, 2013.

[17] L. Namgyal and J. Hall, "Coherent streamwise vortex structure of a three-dimensional wall jet," *Fluids*, vol. 6, p. 35, January 2021.

[18] B. Sim and J. Hall, "Streamwise variation of the unsteady pressure field in the three-dimensional wall jet," in *AIAA Scitech 2020 Forum*, (Orlando, FL, USA), January 2020.

[19] B. Sim and J. Hall, "Proper orthogonal decomposition of the unsteady pressure field in the three-dimensional wall jet," in *Progress in Canadian Engineering. Volume 3*, (PEI, CA), June 2020.

[20] M. Gad-el Hak, *Flow Control: Passive, Active, and Reactive Flow Management*. Cambridge; New York: Cambridge University Press, 2000.

[21] C. L. Perez, J. W. Hall, R. Sagher, and M. N. Glauser, "Towards controlling the three-dimensional wall jet development," in *AIAA 2007-4493*, (Miami, Florida), pp. 1–9, June 2007.

[22] C. L. Perez, R. Sagher, J. W. Hall, and M. N. Glauser, "Controlling the lateral spread of a three-dimensional wall jet," in *1000 Islands Fluids Mechanics Meeting*, (Gananoque, Canada), pp. 1–3, 2007.

[23] A. Glezer and M. Amitay, "Synthetic jets," *Ann. Rev. of Fluid Mech.*, vol. 34, no. 1, pp. 503–29, 2002.

[24] K. Mohseni and R. Mittal, "Synthetic jets: Basic principals," in *Synthetic Jets - Fundamentals and Applications* (K. Mohseni and R. Mittal, eds.), ch. 1, pp. 3–48, Boca Raton, FL, USA: CRC Press, 2014.

[25] D. A. Tamburello and M. Amitay, "Active control of a free jet using a synthetic jet," *Int. J. Heat Fluid Flow*, vol. 29, pp. 967–84, 2008.

[26] A. Glezer, "Some aspects of aerodynamic flow control using synthetic-jet actuation," *Phil. Trans. R. Soc. A*, vol. 369, pp. 1476–1494–29, 2011.

[27] Z. Broučková and Z. Trávníček, "Intermittent round jet controlled by lateral pulse-modulated synthetic jets," *J. Visualization*, vol. 22, no. 3, pp. 459–476, 2019.

[28] F. E. Jørgensen, "How to measure turbulence with hot-wire anemomemters - a practical guide," manual, Dantec Dynamics, 2002.

[29] DANTEC Documentation Department, Scientific Research Equipment Division, "Instruction manual 56c17 CTA bridge," manual, Dantec Dynamics, June 1988.

[30] H. H. Bruun, *Hot-Wire Anemometry*. Walton Street, Oxford, OX2 6DP: Oxford University Press, 1st ed., 1995.

[31] PUI Audio Inc, "APS4812B-LW-100-R 48mm piezo speaker," Data Sheet APS4812B-LW-100-R, PUI Audio Inc, July 2015.

[32] LePage, "Super glue ultra gel™," techincal data sheet, Mississauga, CA, 2015.

[33] Gorilla Glue Company, "Safety data sheet - original Gorilla Glue," safety data sheet, Cincinnati, OH, USA, 2018.

[34] J.-C. Gantet, "Scientific and industrial report," project report, University of New Brunswick, 2009. Under Dr. J. W. Hall's supervision.

[35] C. Meilhan, "Scientific and industrial report," project report, University of New Brunswick, 2010. Under Dr. J. W. Hall's supervision.

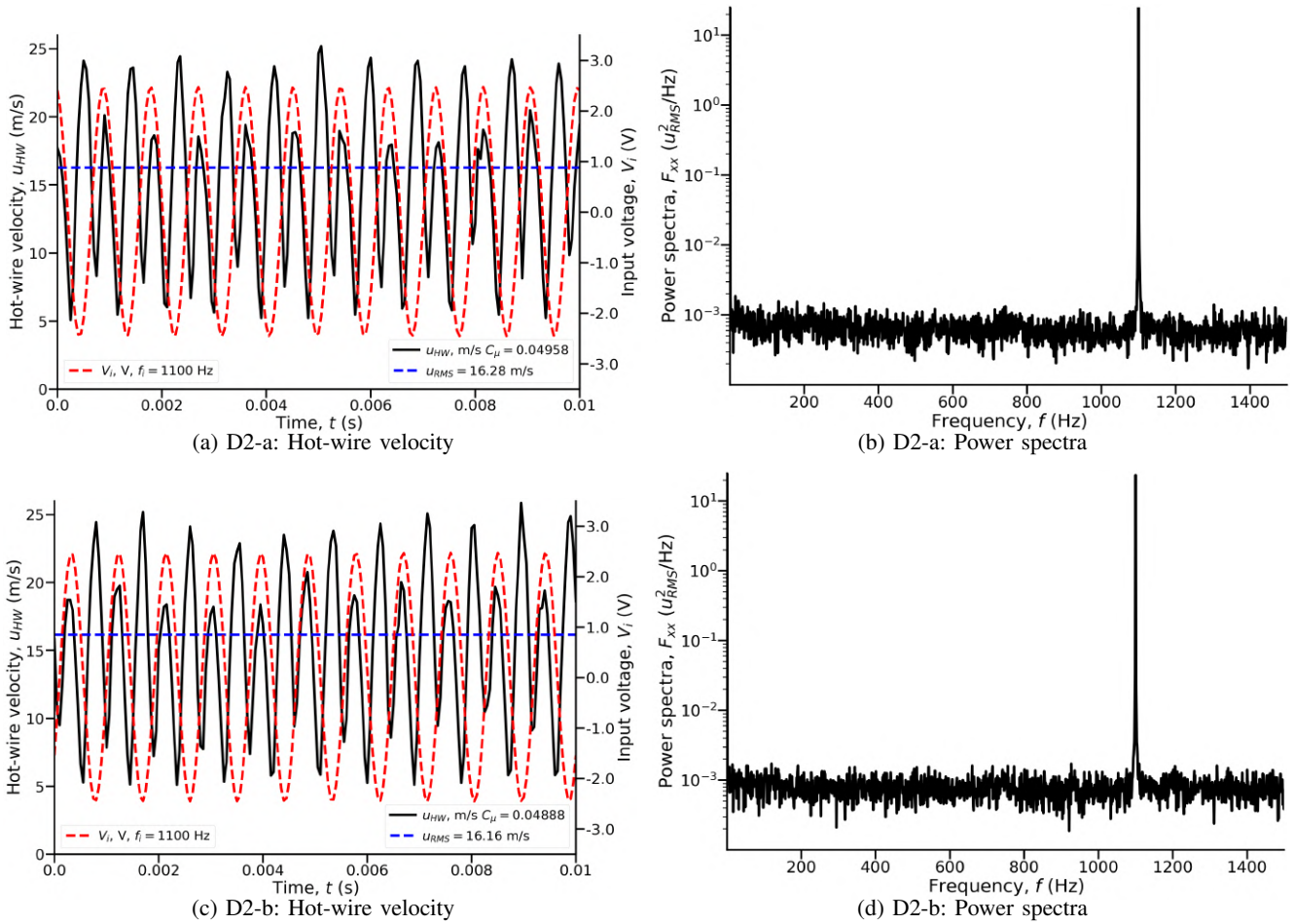

(a) D2-a: Hot-wire velocity

(b) D2-a: Power spectra

(c) D2-b: Hot-wire velocity

(d) D2-b: Power spectra

Fig. 6: Hot-wire velocity measurements and input signals for two D2 synthetic jet actuators and their corresponding power spectra with a sinusoidal input at 1100 Hz..

[36] T. Van Buren, E. Whalen, and M. Amitay, "Synthetic jet actuator cavity acoustics: Helmholtz versus quarter-wave resonance," *J. Vibration Acoustics*, vol. 137, no. 5, 2015.

[37] CUI Inc, "Electret condensor microphone," Data Sheet Part. No. CMC-5044PF-A, CUI Inc, June 2008.

[38] L. N. Cattafesta and M. Oyarzun, "Design of synthetic jets," in *Synthetic Jets - Fundamentals and Applications* (K. Mohseni and R. Mittal, eds.), ch. 2, pp. 49–97, Boca Raton, FL, USA: CRC Press, 2014.

[39] J. T. Pinier, J. M. Ausseur, M. N. Glauser, and H. Higuchi, "Proportional closed-loop feedback control of flow separation," *AIAA J.*, vol. 45, pp. 181–90, January 2007.